Dynamic B0 Shimming in the Heart at 3T

J. A. Stainsby[1], V. Ramanan[2], and G. A. Wright[2]

[1]GE Healthcare, Toronto, Ontario, Canada, [2]Imaging Research, Sunnybrook Health Sciences Centre, Toronto, Ontario, Canada

Introduction: The need for dynamically updating shim gradients during scanning has been recognized recently. This need arises due to the difficulty of correcting for field inhomogeneities found in vivo using global shim values. Recently dynamic shim updating has been shown to benefit multi-voxel spectroscopy[1], and neuro imaging at high fields[2]. Due to the complex field variations that can result from lung-tissue interfaces and localized susceptibility variations near cardiac veins[3], it has been suggested that dynamic shim updating in cardiac imaging would be beneficial[4]. This is particularly true at 3T where these field variations are larger than at 1.5T. This should help to improve the robustness of cardiac imaging at 3T in general, and specifically for sequences that are more sensitive to susceptibility variations such as steady-state free precession and BOLD-sensitive sequences.

Methods: All experiments were performed on a GE 3T Signa scanner (GE Healthcare, Waukesha, WI) scanner equipped with 4.0 G/cm gradients. RF was transmitted and received with a body coil to avoid issues in combining phase information from multiple receivers. First a multi-slice, multi-phase field map sequence was acquired following routine global shimming. Imaging parameters were FOV=34cm, 64x64, 125kHz RBW, 11 cardiac phases, TE=2.0/4.2ms, first order flow compensation enabled. Three axial mid-ventricular slices were acquired in a single 21-second breath hold. Field maps were generated from a 2D phase unwrapped difference image from the 2 TEs. The residual zero and first order shim terms were fit, over manually defined regions of interest containing the RV and LV, using a minimum least squares algorithm and these terms were then fed back into the sequence for a second acquisition, where the center frequency and in-plane linear shim terms were updated dynamically prior to each cardiac phase

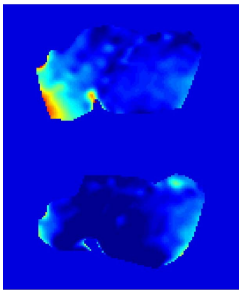

Figure 1: Sample field maps from a single slice and cardiac phase before (left) and after (right) dynamic shim adjustments. The frequency range is –20 Hz (blue) to +200 Hz (red).

Results: A sample field map from one slice at one cardiac phase (trigger delay=290ms) before and after dynamic shim correction is shown in Fig 1. After routine global shimming for the 3-slice prescription, the distribution width that contains 75% of the field values with no correction was 60.3 Hz, after removing up to linear terms the predicted distribution width is 47.9 Hz. Applying up to first order shim corrections dynamically resulted in an actual reduction in distribution width to 54.4 Hz. Given the slice to slice variation in the 0^{th} order term (see Fig 2), differences in breath hold position between acquisitions could account for some of this difference. Plots of the fit zero (center frequency) and in-plane linear shim terms on maps acquired with and without dynamic shim updating are given in Figs 2-4. The mean residual center frequency term across all 3 slices and all 11 cardiac phases after routine global shimming was 28.5 Hz. Following dynamic shimming this dropped to 2.3 Hz. The mean linear shim terms in the L/R and A/P directions after global shimming were –3.35 Hz/cm and 3.05 Hz/cm and we achieved a reduction to –0.19 Hz/cm and 1.15 Hz/cm respectively following dynamic shimming.

Discussion: We have presented dynamic, slice-by-slice and phase-by-phase shimming applied to cardiac imaging at 3T. Following routine global shimming, there are significant residual field variations. Dynamic shimming of the center frequency and linear shim terms was demonstrated to significantly reduce the field variations. Tradeoffs between the spatial/temporal resolution of the field maps and the total acquisition time needs to be investigated further in the context of acquiring field map information for use in dynamic shimming of clinical cardiac studies.

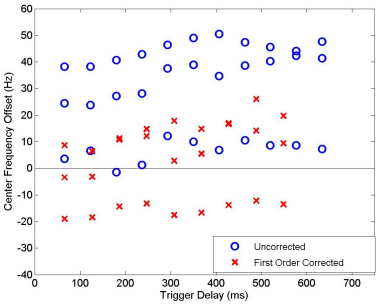

Figure 2: Center frequency offset for all 3 slices and all 11 phases measured after global shimming (uncorrected) and after dynamically updating shims before each cardiac phase.

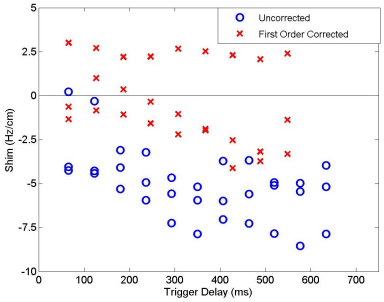

Figure 3: Linear x-shim variation after global shimming (uncorrected, circles) and after dynamically updating shims (x's).

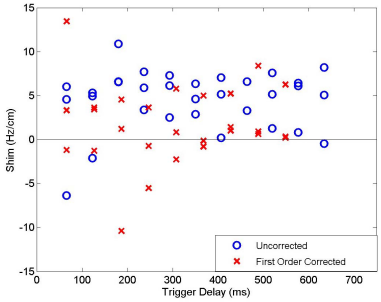

Figure 4: Linear y-shim variation after global shimming (uncorrected, circles) and after dynamically updating shims (x's).

References: [1] K Koch et al, MRM, 57:587, (2007), [2] P van Gelderen et al, MRM, 57:362 (2007), [3] S Reeder et al, MRM, 39:988 (1998), [4] Schar et al, MRM, 51:799 (2004), [5] Koch et al, JMR, 180 (2006)